Center for Advanced Materials

CAM REPORT

Presented at the NATO Advanced Study Institute on Alloy Phase Stability, Crete, Greece, June 14–27, 1987

STRAIN CONTROLLED MORPHOLOGIES IN THE TWO-PHASE STATE

A.G. Khachaturyan

June 1987

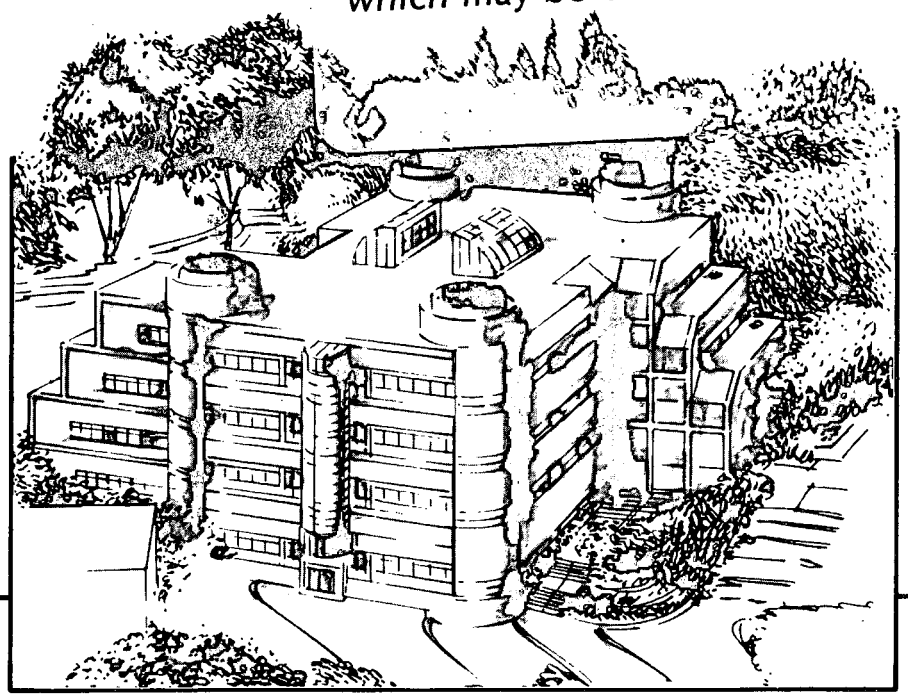

Materials and Chemical Sciences Division

Lawrence Berkeley Laboratory • University of California

ONE CYCLOTRON ROAD, BERKELEY, CA 94720 • (415) 486-4755

Prepared for the U.S. Department of Energy under Contract DE-AC03-76SF00098

DISCLAIMER

STRAIN CONTROLLED MORPHOLOGIES IN THE TWO-PHASE STATE

A.G. Khachaturyan

Center for Advanced Materials,
Lawrence Berkeley Laboratory
and
Department of Materials Science and Mineral Engineering

University of California
Berkeley, California 94720

Lecture Notes

NATO Advanced Study Institute on Alloy Phase Stability
Crete, Greece

June 14-27, 1987

STRAIN-CONTROLLED MORPHOLOGIES OF THE TWO-PHASE STATE

I. INTRODUCTION

Phase transformation in solids usually involve crystal lattice rearrangement with the islands of the new phase inside the parent phase matrix. Crystal lattice mismatch produced by phase transformation is accommodated by elastic displacements generating the elastic strain field within the body. The elastic energy contained in the strain field may contribute considerably to the thermodynamics of the phase transformation, but the main effect of the elastic strain is far beyond the trivial renormalization of elastic energy. Unlike the "chemical" free energy depending only on the volume of phases, the elastic energy also depends on the morphology, shape, dispersion and mutual location of inclusions. In such a case the morphology of the alloy becomes an internal thermodynamic parameter that can be found from the free energy minimization. This, in fact, means that the conventional thermodynamics of phase transformations based on the free energy aditivity should be questioned and validity of certain classical results has to be re-examined. To make more clear how far we can go in revising the theory of phase transformation when elastic energy is involved, it is noteworthy to look at the other cases when the bulk free energy proves to be dependent on morphology. The other cases where this situation takes place are ferromagnets and ferroelectrics whose magnetostatic and electrostatic energy also depend on shape, size and mutual location of domains. This dependence manifests itself, for example, in appearance of the so-called demagnetization factor, and it affects the ground state of ferromagnets. Indeed, the homogeneous single domain state that would

be expected without magnetostatic energy transforms into an array of domains whose size tends to zero if the Bloch energy (surface energy of domain walls) vanishes. It is also known that the repulsive interaction between the similar domains results in the formation of so-called bubble domain structure.

The similar dramatic effects of the morphology on the thermodynamics of a phase transformation could be expected in the case of a transformation with large crystal lattice rearrangement. The specific examples of such effects are formation of platelet precipitates with the specific habit minimizing the strain energy as well as the formation of agglomerates of various orientional variants of the new phase accommodating crystal lattice mismatch and eliminating elastic strain. The latter effect is observed during martensitic transformation, ordering and decomposiition and is a good example of the profound analogy with the magnetic and ferroelectric domain structure.

The intensive studies of the elastic strain effect caused by the other phase coherent inclusions were initiated by the classical works by Eshelby [1] in the fifties who calculated the elastic energy of an ellipsoidal inclusion in an isotropic case. The next step was made in our work [2] and the work by Roitburd [3] where the idea that the elastic strain eneregy minimization can be used for the habit plane determination was first proposed.

The general theory of elastic energy of an arbitrary distributed inclusion in elastically anisotropic medium in the homogeneous modulus case was formulated by Khachaturyan and Shatalov [4] and developed by Wen, Khachaturyan and Morris [5]. The theory was used for analyzing morphology of a single precipitate [6-13] and morphology transformations

of a group of precipitates [4,5,9,14-18]. The exact solution of the elastic problem for an ellipsoidal inclusion in the heterogeneous modulus case and anisotropic crystals was obtained by Lee, Barnett and Aaronson [19].

The main topic of these lectures is the discussion of the application of the elastic theory to practical problems which arise in structural studies of the morphology of two-phase alloys. The consideration will be based on the theory developed for the homogeneous modulus case [2,4] because this approach enables one to treat arbitrary dispersoids using very simple mathematics. The cases where this approximation turns out to be insufficient will be discussed separately. The applied aspects of the theory will be especially emphasized. There are three groups of problems that deserve to be discussed in detail:

1. Morphology of a single coherent precipitate, its habit plane, equilibrium shape, orientational relations and crystal lattice parameters in the constraint state.

2. Shape transformations and morphology instabilities upon coarsening.

3. Strain-induced rearrangement of groups of precipitates upon coarsening.

2. ELASTIC ENERGY AND ELASTIC DISPLACEMENTS INDUCED BY ARBITRARY ARRAY OF COHERENT INCLUSIONS

Following [4] let us consider n types of inclusions that are produced by different crystal lattice rearrangements, for example, the rearrangements generating the different orientational variants of the same phase. These inclusions may be characterized by stress-free transformation strains, $\varepsilon^{\circ}_{ij}(1)$, ..., $\varepsilon^{\circ}_{ij}(p)$, ...$\varepsilon^{\circ}_{ij}(n)$ describing the

macroscopic shape change of the parent phase caused by the respective crystal lattice rearrangements. These inclusions can be produced by means of the four steps of the Eshelby cycle:

1. Cut inclusions from the matrix.

2. Let each inclusion be transformed to a new phase under the stress-free strains $\varepsilon^{\circ}_{ij}(1)$, ...$\varepsilon^{\circ}_{ij}(n)$.

3. Restore the initial shape applying the surface traction to create the opposite sign homogeneous elastic strains, $-\varepsilon^{\circ}_{ij}(1)$, change. The elastic energy required to induce this set of elastic strains is

$$E_{self} = (1/2) \sum_{p=1}^{n} v(p)\ \lambda_{ijkl}\varepsilon^{\circ}_{ij}(p)\ \varepsilon^{\circ}_{kl}(p) \qquad (1)$$

if the elastic moduli of all phases are the same, where λ_{ijkl} is the elastic modulus tensor, i,j,k,l are Cartesian indexes, v(p) the volume of all inclusions of the pth type.

4. Reintroduce restored inclusions in their holes and weld them.

5. Remove the surface traction and allow the inclusions and matrix to relax. The relaxation energy, ΔE, by definition, should be a negative value reducing the energy (1).

The total elastic energy is then

$$E = (1/2) \sum_{p=1}^{n} v(p)\lambda_{ijkl}\varepsilon^{\circ}_{ij}(p)\varepsilon^{\circ}_{kl}(p) + \Delta E \qquad (2)$$

Calculation of the relaxation energy ΔE requires solution of the elasticity problem. The elastic energy (2) is a functional of strain field $\varepsilon_{ij}(r)$ at points r. In the approximation of linear elasticity this functional has the form

$$E = (1/2) \sum_{p=1}^{n} v(p)\lambda_{ijkl}\varepsilon^{\circ}_{ij}(p)\varepsilon^{\circ}_{kl}(q) + (1/2)\int f(\varepsilon_{ij})d^3r \qquad (3)$$

where

$$f(\varepsilon_{ij}) \approx - \sigma^{0}_{ij}(r)\varepsilon_{ij}+\lambda_{ijkl}\varepsilon_{ij}\varepsilon_{kl} \qquad (4)$$

where $\sigma^{0}_{ij}(r)$ and λ_{ijkl} are the first- and second- order expansion coefficients of the local elastic energy $f(\varepsilon_{ij})$ which are material constants. The unusual term in (4), linear in ε_{ij}, appears because in the system with inclusions the stress-free states is not a non-deformed state. The minimization of eq.(3) with respect to elastic displacements (finding mechanical equilibrium) requires solution of the equation of elasticity, $\partial\sigma_{ij}/\partial x_j=0$ where $\sigma_{ij}(r)$ is stress at the point $r=(x_1,x_2,x_3)$. Stress $\sigma_{ij}(r)$ is, by definition, the first variation of (3) with respect to ε_{ij}. Together with (4), it gives

$$\sigma_{ij}(r) = \frac{\delta E}{\delta \varepsilon_{ij}(r)} = -\sigma^{0}_{ij}(r) + \lambda_{ijkl}\varepsilon_{kl}(r) \qquad (5)$$

Let us reveal the physical meaning of the material constants, $\sigma^{0}_{ij}(r)$. At the stress-free state, $\sigma_{ij}(r)=0$, we have by definition of the stress-free state

$$\sigma^{0}_{ij}(r) = \begin{cases} \lambda_{ijkl}\varepsilon^{0}_{kl}(p) & \text{if } r \text{ is inside a particle of the type } p. \\ 0 & \text{otherwise} \end{cases}$$

The latter condition can be rewritten in the condensed form

$$\sigma^{0}_{ij}(r) = \Sigma\, \lambda_{ijkl}\varepsilon^{0}_{kl}(p)\ \tilde{\theta}(p,r) \qquad (6)$$

where $\theta(p,r)$ is the shape function of the precipitates of type (p); it is equal to unity if vector r corresponds to a point within an inclusion of the type p and is 0 otherwise. Introduction of shape function $\tilde{\theta}(p,r)$ is very convenient because they describe spatial distribution of arbitrary inclusions. With definition (6) eq.(5) is

$$\sigma_{ij}(r) = -\sum_{p=1}^{n} \sigma^{0}_{ij}(p)\ \tilde{\theta}(p,r)\ \varepsilon_{ij} + \lambda_{ijkl}\ \varepsilon_{kl} \qquad (7)$$

The elastic equilibrium equation $\partial\sigma_{ij}/\partial x_j=0$ can then be rewritten in the form

$$\lambda_{ijkl}\,\frac{M^2 u_l}{\partial x_j \partial x_k} = \sum_{p=1}^{n} \sigma^{\circ}_{ij}(p)\,\frac{\partial\theta(p,k)}{\partial x_j} \qquad (8)$$

where the strain definition, $\varepsilon_{ij} = (1/2)(\partial u_i/\partial x_j + \partial u_j/\partial x_i)$, was used. Multiplying eq.(8) by the factor $\exp(-ikr)$ and integrating over r yields

$$\lambda_{ijkl}\,k_j k_k\,u_l(k) = -i\sum_{p=1}^{n}\sigma^{\circ}_{ij}(p)\,k_j\,\theta(p,k) \qquad (9a)$$

or in the operator form

$$\hat{G}^{-1}(k)\;v(k) = -i\;\Sigma\;\hat{\sigma}_0(p)\;k\;\theta(p,k) \qquad (9b)$$

where $(G^{-1}(k))_{ij} = \lambda_{ik1j}\,k_k k_1$, $(\hat{\sigma}_0(p))_{ij} = \sigma^{\circ}_{ij}(p)$

$$v(k) = \iiint_{-\infty}^{\infty} u(r)\,\exp(-ikr)\,d^3r$$

$$\theta(p,k) = \iiint_{-\infty}^{\infty} \tilde{\theta}(p,r)\,\exp(-ikr)\,d^3r \qquad (10)$$

In transition from (8) to (9), the boundary conditions on infinity, $u(r) \to 0$ and $\varepsilon_{ij}(r) \to 0$ at $r \to \infty$, were used.

The solution of eq.(9) is

$$v(k) = -i\sum_{p=1}^{n} G(k)\,\sigma_0(p)\,k\,\theta(p,k)$$

or in indices

$$v_i(k) = -i\sum_{p=1}^{\infty} G_{ij}(k)\,\sigma^{\circ}_{jk}(p)\,k_k\,\tilde{\theta}(p,k) \qquad (11)$$

where $G_{ij}(k)=(G(k))_{ij}$ is the matrix reverse to the matrix $(G(k)^{-1})_{ij}=\lambda_{ik1j}k_k k_1$, which, in fact is the Fourier transform of the Green function of elasticity equation. Real displacements, $u(r)$, can be found by the back Fourier transform,

$$u(r)_i = -i\sum_{p=1}^{n}\int\frac{d^3k}{(2\pi)^3}\,G(k)_{ij}\,\sigma^{\circ}_{jk}k_k\,\theta(p,k)\,\exp(ikr) \qquad (12)$$

Substituting (12) to (3) and integrating over r within infinite body results in to the Fourier representation of the elastic energy

$$E = (1/2) \sum_p v(p)\, \lambda_{ijkl}\, \varepsilon^{\circ}_{ij}(p)\, \varepsilon^{\circ}_{kl}(p) \qquad (13)$$

$$-(1/2) \sum_{p,q} \int \frac{d^3k}{(2\pi)^3} \langle k|\sigma_0(p)\, G(k)\, \sigma_0(q)|k\rangle \theta(p,k)\, \theta(q,k)^*$$

where $\langle k|\sigma_0(p)\, G(k)\, \sigma_0(q)|k\rangle = k_i\, \sigma^{\circ}_{ij}(p)\, G_{jk}(k)\, \sigma^{\circ}_{kl}(q) k_l$

The identities

$$\int \theta(p,k)\, \theta(q,k)^* \frac{d^3k}{(2\pi)^3} = v(p)\, \delta_{pq}$$

where δ_{pq} is the Kronecker symbol simplify (13):

$$E = (1/2) \Sigma_{p,q} \int \frac{d^3k}{(2\pi)^3} B(k/k)_{pq}\, \theta(p,k)\, \theta(q,k)^* \qquad (14)$$

where $B(n)_{pq} = \gamma_{ijkl}\, \varepsilon^{\circ}_{ij}(p)\, \varepsilon^{\circ}_{kl}(0 - \langle m|\sigma_0(p) \Omega(n)\, \sigma_0(q)|n\rangle$ and $\Omega(m) = k^{-2} G(k)$. Since the shape function $\tilde{\theta}(p,r)$ whose Fourier transform enters (14) can be a multiconnected function describing an array of inclusions of the type p, eq.(14) may be used for calculation of elastic energy of both, an isolated arbitrary shape particle and groups of particles of different types. Therefore eq.(14) is, in fact, close equation for elastic energy of an arbitrary multiparticle system in an anisotropic matrix in the homogeneous modulus case. This energy is the sum of elastic energies of each isolated particle (self-energy) plus strain-induced pairwise interaction energies between particles.

3. A SINGLE PRECIPITATE IN AN INFINITE BODY

A. Elastic Energy of a Single Precipitate.

Closed equation for elastic energy of an isolated coherent particle in an infinite crystal body can be obtained from (14) as a particular

case. The limit transition to a single particle may be readily done if we assume that the phase transition involves only ne type of the crystal lattice rearrangement mode and if the shape function entering eq. (14) describes a simply-connected region enveloping the new phase particle. Then omitting summation over p in (14) we have a simple equation for the elastic energy.

$$E = 1/2 \int \frac{d^3k}{(2\pi)^3} B(k/k) |\theta(k)|^2 \qquad (15)$$

where

$$B(m) = \lambda_{ijkl} \varepsilon^{\circ}_{ij} \varepsilon^{\circ}_{kl} - n_i \sigma^{\circ}_{ij} \Omega_{jk}(m) \sigma^{\circ}_{kl} n_l \qquad (16)$$

$n=k/k$, ε°_{ij} is stress-free transformation strain, $\sigma^{\circ}_{ij}=\lambda_{ijkl}\varepsilon^{\circ}_{kl}$, $\Omega_{jl}(m)=k^{-2} G_{jl}(k)$ is the tensor inverse to $\Omega^{-1}_{jl}(m) = \lambda_{jikl} n_i n_k$, $B(m) \geqslant 0$,

$$|\theta(k)|^2=|\int\theta(r) \exp(-ikr)\, d^3r|^2=|\int \exp(-ikr)\, d^3r|^2 \qquad (17)$$

where integration is carried out over the particle volume V. Equation (17), in fact, yields the Laue interference function describing diffraction on the particle. It is noteworthy that the last term in integrand of (15), B(m), depends on the elastic constants and crystal lattice mismatch only, being a material characteristic, while the second term, $|\theta(k)|^2$, describes the geometry of inclusion only.

For simple shapes we have the following functions for $|\theta(k)|^2$:

$$|\theta(k)|^2 = \frac{\sin^2 k_x a/2}{(k_x/2)^2} \frac{\sin^2 k_y b/2}{(k_y/2)^2} \frac{\sin^2 k_z c/2}{(k_z/2)^2} \qquad (18a)$$

for a parallelopiped with the edge lengths a,b,c, $k=(k_x k_y k_z)$,

$$|\theta(k)|^2 = V^2 \frac{3 \sin\mathfrak{f}(k) - \mathfrak{f}(k) \cos\mathfrak{f}(k)]^2}{(\mathfrak{f}(k))^3} \qquad (18b)$$

for an ellipsoid where $\mathfrak{f}(k)^2=L_{ij}k_i k_j$, L_{ij} is the tensor inverse to L^{-1}_{ij} that determines the standard form of the ellipsoid surface, $L^{-1}_{ij}x_i x_j=1$. The eigenvalues of L_{ij} are squares of the ellipsoid semiaxes, a^2,b^2,c^2.

The ellipsoid model is especially interesting since, as was shown by Eshelby [1] for isotropic elasticity and by Valpole [20] and Willis [21], for anisotropic elasticity, elastic strain inside an ellipsoidal inclusion (eigenstrain) is always homogeneous.

Equation (15) contains the Eshelby solution for an ellipsoid in the homogeneous modulus case as a particular case [22]. If the shape function (18b) is used and the limit transition to isotropic elasticity is made,

$$\lambda_{ijkl} \rightarrow \delta_{ij}\,\delta_{kl}\,2\mu\,(\nu/1-2\nu) + \mu(\delta_{ik}\delta_{jl} + \delta_{il}\delta_{jk})$$

where μ is the shear modulus, ν is the Poisson's ratio, eq. (15) is reduced to the Eshelby solution [1].

B. Optimal Shape and Habit at the Low Interphase Energy Limit.

This problem can be solved minimizing elastic energy (14) at the fixed value of the precipitate volume V.[2] Since $B(\mathbf{m})$ and $|\theta(\mathbf{k})|^2$ are always positive

$$E = 1/2 \int \frac{d^3k}{(2\pi)^3}\, B(\mathbf{m})\, |\theta(\mathbf{k})|^2 \geqslant 1/2\ (\min B(\mathbf{m}))$$

$$\times \int |\theta(\mathbf{k})|^2 \frac{d^3k}{(2\pi)^3} \qquad (19)$$

where min $B(\mathbf{m})$ is the minimum value of $B(\mathbf{m})$. With the identity

$$\int |\theta(\mathbf{k})|^2 \frac{d^3k}{(2\pi)^3} = V$$

inequality (19) is

$$E = 1/2 \int \frac{d^3k}{(2\pi)^3}\, B(\mathbf{k}/k)\, |\theta(\mathbf{k})|^2 \geqslant 1/2\ (\min B(\mathbf{m}))\ V \qquad (20)$$

where the right side of (20) is the lowest possible limit for the elastic energy at a given volume.

Let us introduce the unit vector n_0 providing the minimum of $B(n)$:

$$B(n_0) = \min B(n) \tag{21}$$

For an infinitely thin and infinitely extended platelike inclusion with the habit plane minimal to n_0, the function $|\theta(k)|^2$ differs from zero only within infinitely thin and infinitely long rod in k-space along n_0 (this is a well known result from the diffraction theory; diffraction from plate yield rod in reciprocal space minimal to the habit plane). In this case the inequality (20) becomes equality. Therefore the minimum elastic energy is attained if an inclusion is "rolled out" into the infinitely thin plate with the habit normal to the vector n_0 minimizing $B(n)$. The elastic energy then is

$$E = E_{bulk} = (1/2) \min B(n)\ V = (1/2)\ B(n_0)V \tag{22}$$

This strain energy (22) is proportional to the inclusion volume, V.

C. Bulk Energy of an Inclusion with Invariant Plane Strain Crystal Lattice Rearrangement.

The case of an invariant plane transformation strain plays an especially important role in the theory of phase transformations. For example, the idea of invariant plane strain is basic for the entire crystallographic theory of martensitic transformation which resulted in remarkable achievements in understanding the crystallography of this transformation. The theoretical results obtained above enable us to realize what is the reason behind this.

According to the crystallographic theory, the habit plane of a martensitic crystal is an invariant plane strain. It will be shown below that this directly follows from eq. (22) as a result of the minimization of the elastic energy (15).

The invariant plane strain has always a form of a diadic product

$$n^{o}_{ij} = \varepsilon_o l_i n^{o}_j \qquad (23)$$

where 1 is a unit vector along the displacement direction, n^{o} is a unit vector normal to the invariant plane.

Substituting (23) for ε^{o}_{ij} to eq. (16) for B(n) yields

$$B(n) = \varepsilon_o^2 \left[\lambda_{ijkl} l_i l_k n_j n^{o}_l - \lambda_{ijsp} n^{o}_i n^{o}_p l_s \, \Omega_{jt}(n) \lambda_{tmqr} \, n^{o}_r n^{o}_m l_q\right] \qquad (24)$$

One may see that at $n=n_o$ $B(n_o)=0$ since by definition of $\Omega^{-1}(n)$ $\lambda_{tmqr} \, n^{o}_r \, n^{o}_m = \Omega^{-1}(n^{o})_{iq}$. Therefore the bulk energy (21) vanishes. We have the following simplification in (24)

$$\Omega_{jt}(n_o) \, \lambda_{tmqr} n^{o}_r n^{o}_m = \Omega_{jt}(n_o) \, \Omega^{-1}(n_o)_{tq} = \delta_{jq}$$

Using the latter in (23) we get $B(n_o) = 0$. We have proved the result that in the case of an invariant plane transformation strain, the minimum of the bulk elastic energy equal to zero is attained when the inclusion is a plate whose habit plane coincides with the invariant plane. This exceptional situation when the choice of the optimal habit plane may eliminate the most substantial volume dependent positive elastic energy makes the case of the invariant plane strain so important. For example, one substantial conclusion can be immediately made: <u>if any group of new phase coherent precipitates may rearrange itself so that a plate-like aggregate of various orientational variants of the precipitate phase gives the macroscopic shape change described by an invariant plane strain, it will do this to eliminate the volume dependent elastic strain</u>. This conclusion gives us the direction of strain-induced coarsening of such precipitate systems. The typical examples of such systems are tetragonal precipitates in a cubic phase matrix that ultimately form the martensite-type structure with the surface relief

and habit plane determined by the conventional crystallographic theory of martensitic transformation.

D. Habit Plane of Tetragonal and Hexagonal Precipitates.

Equation (21) for the habit plane was solved for the thin plate tetragonal plate-like inclusion in a cubic matrix in [12] and for a hexagonal inclusion in [11].

The solution for a tetragonal inclusion gives two types of the habit, (h01) for the negative elastic anisotropy $c_{11}-c_{12}-2c_{44} < 0$, and (hhl) for the positive anisotropy $c_{11}-c_{12}-2c_{44} > 0$.

(i) If $c_{11}-c_{12}-2c_{44} < 0$, the normal to the habit plane, $\mathbf{n}_o$, is $\mathbf{n}_o = (\sin\theta, 0, \cos\theta)$ where

$$\cos^2\theta = \begin{cases} 0 & \text{if } -\infty < t < -[(c_{11}/c_{12})+1] \text{ and } 1 < t < \infty \\ 1 + \dfrac{c_{11}+2c_{12}}{c_{11}+c_{12}} \dfrac{t}{1-t} & \text{if } -[(c_{11}/c_{12})+1] < t < 0 \\ 1 & \text{if } 0 \leqslant t < 1 \end{cases} \qquad (25a)$$

where $t = \varepsilon^o_{11}/\varepsilon^o_{33}$, ε^o_{11} and ε^o_{33} are non-zero components of the stress-free transformation strain ε^o_{ij} (all other components are zero).

(ii) If $c_{11}-c_{12}-2c_{44} > 0$, the normal to the habit plane is $\mathbf{n}_o = ((1/\sqrt{2})\sin\theta, (1/\sqrt{2})\sin\theta, \cos\theta))$

where

$$\cos^2\theta = \begin{cases} 0 & \text{if } -\infty < t < t_1 \\ 1 - 2\dfrac{(\xi+2)(c_{11}+2c_{12})t}{\xi(c_{11}+2c_{12})(2t-1) + 4(c_{11}+c_{12})(t-1)} & \text{if } t_1 < t < 0 \\ 1 & \text{if } 0 \leqslant t \leqslant t_2 \\ \xi\dfrac{(c_{11}+2c_{12}) + 4c_{11}(1-t)}{\xi(c_{11}+2c_{12})(1+2t)} & \text{if } t_2 < t < t_3 \end{cases} \qquad (25b)$$

where $t_1 = -(c_{11}/c_{12})-1 - \xi\dfrac{(c_{11}+2c_{12})}{4c_{12}}$, $t_2 = \dfrac{2c_{11}}{2c_{11}+\xi(c_{11}+2c_{12})}$

$$t_3 = 1 + \xi\frac{c_{11}+2c_{12}}{4c_{44}}, \quad t_1 < t_2 < t_3$$

It follows from eq.(25a) and (25b) that for a cubic precipitate in a cubic matrix (when t=1), the habit plane is (001) if $c_{11}-c_{12}-2c_{44} < 0$ and is (111) if $c_{11}-c_{12}-2c_{44} > 0$.

Similar calculations were made by Mayo and Tsakalakos for precipitates of orthorhombic and hexagonal phase [11]. They derived explicit analytical expression for B(n) in terms of crystal lattice misfit and elastic constants of the hexagonal phase. Minimizing this equation with respect to n they were able to predict the habit of precipitates. This approach was applied to Al-Mg-Zn alloy with Zn/Mg ratio between 2.5 and 7, and the total Zn content less than 20 wt pct. The predicted $\{111\}_{fcc}$ habit plane of the η' phase in the fcc Al-based matrix is in agreement with electron microscopic observations [23,24].

E. Elastic Energy of Finite Thin Plate Inclusions.

Finite thickness of a precipitate with the optimal habit normal to n_o should result in a positive correction to eq. (21), ΔE_{edge}. Mathematically it is associated with the fact that the rod in k-space where $|\theta(k)|^2$ does not vanish for a finite thickness platelet has finite thickness and finite length. They are of the order of magnitude $2\pi/L$ and $2\pi/D$, respectively where L and D are typical length and thickness of the plate-like precipitate. In this case, the energy correction to (21) is positive because integration over k in (15) is carried out over k space region where B(k/k) does not assume its minimum value $B(n_o)$. Therefore the correction, ΔE_{edge}, is of the order of $\Delta E_{edge}/E_{plate} \sim (D/L)^2$, i.e.,

$$\Delta E_{edge} \sim E_{plate}\,(D/L)^2 = \lambda\varepsilon_o^2(DL^2)(D/L)^2 \sim \lambda(\varepsilon_o D)^2\, L \sim \lambda(\varepsilon_o D)^2\, P$$

where P is the platelet perimeter. The physical meaning of the correction is quite clear. It is caused by the crystal lattice mismatch on

the edges of the inclusion along its perimeter. The energy correction, ΔE_{edge}, can be interpreted as "string" energy with the line tensions $\sim\lambda(\varepsilon_o D)^2$. In fact this energy can be attributed to a dislocation loop with the Burgers vector $b=\sim\varepsilon_o D$ enveloping the precipitate in its habit plane. Accurate calculations of the energy ΔE_{edge} for a tetragonal precipitate in the cubic matrix gives

$$\Delta E_{edge} = \beta(D^2/4\pi)\ \ln(L/D)\ P$$

where

$$\beta = \frac{(2c_{12}\varepsilon^{\circ}_{11}+c_{11}\varepsilon^{\circ}_{33})^2}{c_{11}}\left[\frac{\xi\ c_{11}+c_{12}}{c_{11}} - \frac{c_{11}(1+\alpha_1^2)-2c_{12}\alpha_1 - 2(\alpha_1+1)}{c_{44}}\right]$$

ε°_{33} and N°_{11} are crystal lattice mismatch along the tetragonality axis and in the normal to the plane (001), respectively, $\xi=(c_{11}-c_{12}-2c_{44})/c_{44}$ is the anisotropy parameter [20]. In the case of a cubic precipitate in a cubic matrix ($\varepsilon_{11}=\varepsilon_{33}=\varepsilon_o$),

$$\beta = -\frac{(c_{11}+2c_{12})^2\ \varepsilon_o^2\ \xi(c_{11}-c_{12})}{c_{11}^2}$$

It was shown that in a general case of arbitrary symmetry phase the edge energy of a plate-like precipitate is

$$\Delta E_{edge} = (D^2/4\pi)\ \ln L/D \int\left[\beta_1 \frac{(dy/dx)^2}{1+(dy/dx)^2} + \beta_2 \frac{1}{1+(dy/dx)^2}\right] dl$$

where integration is taken over the contour $y=y(x)$ enveloping the precipitate in the habit plane, dl is the contour length element, β_1 and β_2 are second order expansion coefficients with respect to $n-n_o$. The minimization of the ΔE_{edge} energy with respect to the shape in the habit plane described under the additional condition of conservaation of its area in the habit plane, $S=\int y(x)\,dx$, gives the Lagrange equation for $y=y(x)$. The solution of this equation results in the forms presented in Fig. 1.

F. Crystal Lattice Parameters and Crystal Lattice Rotation in Constraint Plate-Like Inclusion.

In the case of a single inclusion eq.(12) for elastic displacements yields

$$u(r) = i \int (d^3k/(2\pi)^3)\ \hat{G}(k)\ \hat{\sigma}^{\circ} k\ \theta(k)\ \exp(-ikr) \qquad (26)$$

The coordinate derivative $\partial u_i/\partial x_j$ gives the distortion tensor, $u_{ij}(r)$,

$$u_{ij}(r) = \partial u_i/\partial x_j = \int (\hat{G}(k)\hat{\sigma}_o k)_i k_j\ \theta(u)\exp(-ikr)\ d^3k/(2\pi)^3$$

Since by definition of the Green function G(k),

$$G(k) = \frac{1}{k^{-2}\ \hat{\Omega}\ (n)} \qquad \text{where } n = k/k,$$

$$u_{ij}(r) = \int n_j (\hat{\Omega}\ (\sigma n)\ \hat{\sigma}_o n)_i\ \theta(k)\ \exp(-ikr)\ d^3k/(2\pi)^3 \qquad (27)$$

In the case of a plate-like inclusion eq. (27) is substantually simplified because the Fourier transform of its shape functions, $\theta(k)$, does not vanish only within the thin and extended rod in k-space emerging from the origin, k=0, along the direction n_o normal to the habit. Then

$$u_{ij}(r) \simeq n_j^{\circ} (\hat{\Omega}\ (n_o)\ \hat{\sigma}_o n_o)_i \int \theta(k)\ \exp(-ir)\ d^3k/(2\pi)^3 \qquad (28)$$

with accuracy of the ratio D/L<<1. The integral in the right hand part of (28) is the back Fourier transform of $\theta(k)$ and therefore, by definition, is equal to $\theta(r)$. Taking the latter into account we have

$$u_{ij}(r) = S_i(n^{\circ})_i n_j^{\circ} \theta(r) = \begin{cases} u_{ij}^{*} = S(n^{\circ})_i n_j^{\circ} & \text{if r is inside the inclusion} \\ 0 & \text{otherwise} \end{cases} \qquad (29a)$$

where

$$S(n^{\circ}) = \hat{\Omega}\ (n_o)\hat{\sigma}_o n^{\circ} \qquad (29b)$$

For the cubic -> cubic phase transformation $\sigma_{ij}^{\circ} = (c_{11} + 2c_{12})\ \varepsilon_o \delta_{ij}$. It has been shown in section 3D that if $c_{11}-c_{12}-2c_{12} < 0$, the habit is (001), $n_o = (001)$ and thus $\sigma_o n_o = (c_{11} + 2c_{12})\varepsilon_o n_o$. On the other hand $\Omega\ (n_o)n_o = 1/c_{11}\ n_o$ if $n_o = (001)$. Using these relations gives

$S(n_o) = \Omega\ (n_o)\ \sigma_o n_o = \varepsilon_o n_o (c_{11}+2c_{12})/c_{11}$. Then the eignstrain u^*_{ij} in eq.(29) can be rewritten as

$$u^*_{ij} = S(n_o)_i n^o_j = \varepsilon_o n_i n_j (c_{11} + 2c_{12})/c_{11}$$

$$= \varepsilon_o ((c_{11}+2c_{12})/c_{11}) \begin{pmatrix} 000 \\ 000 \\ 001 \end{pmatrix} \qquad (30)$$

Therefore a constraint coherent (001) platelet precipitate of a cubic phase has always a strain-induced tetragonality described by (30), the axial ratio being $(c/a)=1+\varepsilon_o(c_{11}+2c_{12})/c_{11}$. If $c_{11}-c_{12}-2c_{44} > 0$, $n_o = 1/\sqrt{3}$ (111) and the similar calculation yields

$$u^*_{ij} = \frac{1}{3} \frac{c_{11} + 2c_{12}}{c_{11} + 2c_{12} + 4c_{44}} \varepsilon_o \begin{pmatrix} 111 \\ 111 \\ 111 \end{pmatrix}$$

Therefore a constraint coherent (111) platelet of a cubic phase has always strain-induced rhombohedricity.

Equation (29) leads us to the following important conclusions:

1. The distortion within a platelike inclusion, u^*_{ij}, is homogeneous. Distortion outside the inclusion in the matrix asymptotically vanishes when $D/L \to 0$.

2. Since almost all elastic strain is concentrated within the platelet, the total elastic energy is not sensitive to the elastic moduli of the matrix. Therefore eq.(22) for elastic energy of a platelet derived in the homogeneous modulus case is nevertheless asymptotically correct also in the heterogeneous modulus case if the elastic moduli, λ_{ijkl} in (22) are substituted by the elastic moduli of the precipitate.

3. The total distortion within a constraint platelet transforms the matrix lattice to the constrain preceipitate lattice is always an invariant plane strain, the invariant plane normal to n_o coinciding with the

habit plane. Therefore any crystal lattice translation in the habit plane of a constraint precipitate exactly coincides with the corresponding translation in the matrix plane parallel to the habit.

4. The crystal lattice rotation caused by fitting two different lattices along the habit plane is described by the asymmetric part of the distortion tensor u^*_{ij}:

$$\omega^*_{ij} = (1/2)\ [u_{ij}-u_{ji}) = (1/2)\ [S(m_o)_i\ n^o_j - n^o_i S(m_o)_j]$$

or by the rotation vector

$$\omega = 1/2\ (S(m_o) \times n^o)$$

The direction of ω is the rotation axis direction, the absolute value of ω is the rotation angle.

G. Needle-Like Precipitates.

As was shown above that the elastic energy assumes its minimum for a platelike precipitate whose habit is normal to the vector n^o minimizing B(n). Mayo and Tsakalakos [11] have shown that this is not always the case. Needle-like precipitates may be more stable if the minimum of the function B(n) is degenerated with respect to n lying in the plane. Such a situation may be epected if B(n) has the cylindrical symmetry with respect to n.

If B(n) has a cylindrical symmetry with respect to an axis directed along the direction e, the function B(n) depends on the scalar product ne: B(n) = B(ne). In the case of interest when B(n) assumes its absolute minimum at n normal to the symmetry axis (at (ne)=0), one may expand B(n) in a power series of

$$(ne):\quad B(n) = \min B(n) + \beta(ne)^2 + \ldots \qquad (31)$$

substituting (31) to (27) and using the identity

$$\int|\theta(k)|^2\ d^3k/(2\pi)^3 = V$$ yields

$$E \cong (1/2)\ \min B(\mathbf{n})V + (1/2)\ \beta\int(\mathbf{ne})^2|\theta(\mathbf{k})|^2 d^3k/(2\pi)^3 \qquad (32)$$

The energy (32) is minimized for a needle along the direction e because the function $|\theta(n)|^2$ for a needle does not vanish within thin extended plate in u space normal to the needle axis e where ne = 0. Estimation of the integral in (33) for a needle along the axis e describing strain concentration near the needle tip yields [22]

$$\Delta E_{edge} = (1/2)\ \beta\int(\mathbf{ne})^2\ |\theta(\mathbf{k})|^2\ d^3k/(2\pi)^3 \cong (1/2)\ \beta R_0^3\ 4/3\pi$$

where $\beta \sim \lambda\varepsilon_0^2$, R_0 is a needle radius.

For a thin and long needle the correction to the bulk energy ΔE_{edge} is much smaller than the corresponding correciton $\Delta E_{edge} \sim \lambda\varepsilon_0^2 DL$ for a thin plate. The bulk energy term (22) for a plate is the same as for a needle but the energy corrections ΔE_{edge} for a needle is much smaller than that for a plate (the first is proportional to R_0^3 while the second to D^2L). The calculations similar to that for a plate-like precipitate [22] give for a needle the following result:

1. Strain inside a coherent needle-like precipitate parallel to the direction e is homogeneous and has the form

$$\varepsilon^*_{ij} = (1/2)\ \alpha(\delta_{ij} - e_ie_j)$$

For a particular case of a tetragonal elastically isotropic precipitate $\alpha = (\varepsilon^\circ_{11} + \nu\varepsilon^\circ_{33})/(1+\nu)$, where ν is the Poisson ratio, ε°_{33} and ε°_{11} are the tetragonal stress-free strains along and perpendicular to the tetragonal axis.

2. Crystal lattice translations of constraint needle-like precipitate exactly coincide with the corresponding translations of the matrix phase. The latter can be seen from the equation

$$r'_i = [\delta_{ij} + \alpha(\delta_{ij} - e_ie_j)]\ r_0e_j = r_0e_i$$

which shows that the length r_0e along the direction e does not change.

Now a few words concerning cylindrical degeneration of B(n). Analysis of equation (16) for the function B(n) shows that the function B(n) may be cylindrically degenerated with respect to n in the cases of the cubic—tetragonal phase transitions in an alloy based on almost isotropic cubic solvent (Al, Nb, Mo, W and so on) as well as for a cubic—hexagonal, cubic—trigonal and hexagonal—hexagonal phase transitions in anisotropic alloys. The cylindrical degeneration is not sufficient however, for a needle to be formed. It occurs when the minimum of B(n) is degenerated with respect to any n belonging to the phase normal to the cylinder axis. This puts a certain constraint on the transformaiton strain and elastic anisotropy.

Concluding this section two important points should be emphasized:

1. Formation of needles can be expected not only in the case of the cylindrical degeneration of the function B(n). Needles can also be stabilized by the interphase energy. Balance between elastic and interphase energy may produce the preferential needle-like shapes as an intermediate form during cooling a precipitate from a spheroid to platelet.

2. The function B(n) is the Fourier transform of interaction energy of two precipitates in the long-distant limit. In the case of the cylindrical degeneration when $B(n) = \min B(n) + \beta(ke)^2/k^2$, the back Fourier transform gives this interaction V(r) in the form of the dipole-dipole interaction

$$V(r) = e_i e_{ij} \beta(\delta_{ij}/r^3 - 3(r_i r_j/r^5) = \beta\ (1/r^3 - 3(re)^2/r^5)$$

where the coefficient β plays the role of the dipole moment magnitude. This fact will be discussed later in connection with the analogy between

elastic shain and magnetostatic energy of magnets and electrostatic energy of ferroelectrics.

4. SHAPE TRANSFORMATIONS OF A CUBIC PHASE PRECIPITATE IN A CUBIC MATRIX UPON COARSENING

As was mentioned above the equilibrium shape of a precipitate is a result of competition between the elastic and interphase energies. Equation (15) enables one to evaluate the elastic energy of an arbitrary shape precipitate while the interphase energy may be assumed to be equal to the product of surface tension coefficient, γ, and interphase area, S, if the interphase tension is isotropic, i.e.

$$E = E_{elast} + E_s \tag{33}$$

where

$$E_s = \gamma S$$

is the interphase energy, and the elastic energy, E_{elast}, is given by eq.(15). Let us consider the cubic-to-cubic phase transformation in the case of the negative elastic anisotropy, $c_{11}-c_{22}-2c_{44} < 0$.

Then integration in (15) yields the elastic energy in the form

$$E_{elast} \cong E_0 V + E_1 \eta V \tag{34}$$

where $E_0 = \varepsilon_0^2 (c_{11} + 2c_{12})(c_{11}-c_{12})/c_{11}$, E_0V is the elastic energy of an infinite thin plate of the volume V with the optimal (001) habit, and

$$E_1 = \frac{(c_{11} + 2c_{12})^2}{2} \quad \frac{(2c_{44} + c_{12}-c_{11})}{c_{11}(c_{11}+c_{12}+2c_{44})} \quad \varepsilon_0^2$$

The dimensionless coefficient η depends on the shape of the precipitate rather than its volume.

The values of the coefficient η in eq.(34) for different shapes are given in Table 1.

TABLE 1

Shape	η
Sphere	0.7087
Cube	0.5580
Needle	0.4692
Thin Plate	0

The total energy (33), elastic and interphase, is thus,

$$E = E_0 + E_1 V\eta + \gamma S$$

or in the reduced form

$$[(E-E_0V)/E_1V] = \eta + \frac{\gamma S}{V} = \eta + \frac{r_0}{a} \qquad (35)$$

where

$$r_0 = \gamma/E_1 \qquad (36)$$

is the material constant with dimension of length, volume-to-surface ratio, $a = V/S$, in a typical particle size, characterizing its degree of coarsening.

Comparing the reduced energy (35) for the various shapes versus the ration r_0/a characterizing the degree of coarsening, the critical transition size from one shape to another can be found. The size a is related to the particle volume V by the following relations:

for a sphere $\quad a = (V/S) = (4/3)(3/4\pi)^{1/3}V^{1/3} \simeq 0.83V^{1/3}$

for a cube $\quad a = (1/6)V^{1/3} \simeq 0.1666V^{1/3}$

for an octahedron $\quad a = (4^{1/3}\sqrt{3}/4)V^{1/3} \simeq 0.69V^{1/3}$

for a tetrahedron $\quad a = (4^{1/3}\sqrt{3}/2)V^{1/3} \simeq 0.35V^{1/3}$

Therefore comparing the reduced energies (35) for a spheroid,

$$(E-E_0V)/E_1V = 0.708 + 1.20\ r_0 / \sqrt[3]{V},$$

and for a cuboid

$$(E-E_0V)/E_1V = 0.07 + 6\,\eta_0 / \sqrt[3]{V},$$

one can see that a spheroidal inclusion is more stable at $\sqrt[3]{V} \leqslant 7.6\ r_0$ and a cuboid precipitate becomes more stable upon coarsening when $\sqrt[3]{V} \geqslant 7.6\ r_0$.

In the case of positive anisotropy, $c_{11}-c_{12}-2c_{44} > 0$, $B(\mathbf{n})$ assumes minimum value at $\mathbf{n} = \mathbf{n}_0 = (1/\sqrt{3}, 1/\sqrt{3}, 1/\sqrt{3})$ and thus the lowest elastic energy is attained for a platelet with the (111) habit. We can also assume that an optimal polihedron which is formed from a spheroid during its coarsening should be faceted by the optimal (111) planes only. Such a polihedron is either octahedron or tetrahedron.

Elastic energy of an octahedron given by integrating eq. (34) was calculated by Tsakalakos.

3. APPLICATIONS

A. GP Zones in Al-Based Alloys.

X-ray and electron microscopic studies have shown that aging of some supersaturated alloys results in the formation of so-called GP zones, small segregations of atoms that later develop into metastable or stable precipitate phase. A GP zone may be either equiaxial (Cu-Co, Al-Zn, Al-Ag etc.) or platelike (Al-Cu, Cu-Be) shapes.

Formation of GP zones can be well understood if they are regarded as new phase precipitates which are formed as a result of isomorphic decomposition occurring according to metastable diagrams with miscibility gap. If the initial solid solution has the cubic lattice, such a decomposition results in atomic redistribution over crystal lattice sites of this lattice and formation of cubic phase precipitates enriched by solute atoms within the cubic phase matrix. Then theoretical results

formulated above may be applied to predict morphology and the structure of GP zones.

Since both phases have the same crystal lattice but different composition, the stress-free transformation shain is a pure dilatation:

$$\varepsilon^{o}_{ij} = \varepsilon_0 \delta_{ij} = (da/adc)\ (c_p - c_m)\delta_{ij} \qquad (37)$$

where da/adc is the concentration coeffeicient of the crystal lattice expansion, c_p and c_m are atomic fractions of solute atoms in the precipitate and matrix, respectively.

a. GP Zones in Al-Cu Alloys

In Al-Cu alloys crystal lattice mismatch is very big. The concentration coeffeicient of the crystal lattice expansion is about 10%:

$$da/adc_{Cu} = -0.091$$

For such a large mismatch the plate-like morphology should be expected. Since $c_{11} - c_{12} - 2c_{44} < 0$ for Al ($c_{11} = 1.068 \times 10^{12}$, $c_{12} = 0.607 \times 10^{12}$, $c_{44} = 0.282 \times 10^{12}$ dn/cm^2, the minimum of B(m) falls on the vector n_o = (001). This means that coherent precipitates should have {100} habit.

According to Gerold [25] a GP zone in Al-Cu alloy is a sole plane (001) of Cu atoms (Fig. 2). This habit is in accordance with the above theoretical predictions. Recent electron microscopic observations seems to confirm this.

Let us estimate the distance between the Cu filled (001) plane and the nearest se planes. According to (30) for a plate-like precipitate of a cubic phase in the cubic matrix with the (001) habit

$$\sigma_0 n_0 = (c_{11} + 2c_{12})\varepsilon_0 n_0 = (c_{11} + 2c_{12})(da/adc)\ (c_p - c_m) n_0$$

$$\Omega(n_0) = (1/c_{11})\ n_0$$

Therefore

$$S(n_0) = \Omega(n_0)\sigma_0 n_0 = \frac{c_{11} + 2c_{12}}{c_{11}} \left(\frac{da}{adc}\right) (c_p - c_m) n_0$$

and the transformation strain (30) within the constrain (001) plate-like precipitate is

$$u^*_{ij} = S(m^o)_i n^o_j = \frac{c_{11} + 2c_{12}}{c_{11}} \left(\frac{da}{adc}\right) (c_p - c_m)\, n^o_i n^o_j =$$

$$= \frac{c_{11} + 2c_{12}}{c_{11}} \frac{da}{adc} (c_p - c_m) \begin{pmatrix} 000 \\ 000 \\ 001 \end{pmatrix} \qquad (38)$$

It follows from (38) that the total strain within a constraint platelet precipitate with the (001) habit transforms its cubic lattice into a tetragonal one. This is the stress-induced tetragonality. The displacement of Al (001) plane nearest to the Cu (001) plane toward the Cu (001) plane produced by eigenstrain u^*_{ij} given by (37) is

$$u = u^*_{33}\, a_{Al}/2 = c_{11} + 2c_{12}/c_{11}\ (da/adc_{Cu})(c_p - c_m)a_{Al}/2 \qquad (39)$$

where a_{Al} is the Al crystal lattice parameter and $a_{Al}/2$ is the interplanar distance for a (001) plane.

The GP zone may be regarded as a plate-like precipitate whose thickness is equal to 2 interplanar distances (D = a). Half crystal lattice sites of such a precipitate are filled by Cu atoms and the other half by Al atoms. Therefore, we may assume that $c_p = 1/2$. Since matrix does not have Cu atoms, $c_m = 0$. Using the latter in eq.(38) together with $(da/adc) \simeq -0.091$ and Al lattice elastic constants we have

$$u = \frac{c_{11} + 2c_{12}}{c_{11}} \left(\frac{da}{adc}\right) (1/2)\, \frac{a_{Al}}{2} = \frac{1.068 + 2 \cdot 0.607}{1.068} \cdot (-0.091)\, \frac{4.041}{4} \simeq -0.196\text{A}^\circ$$

The best fit between calculated and observed x-ray diffuse scattering has been obtained when displacement of the Al (001) plane toward the nearest (001) Cu plane is $u \simeq -0.2\text{A}^\circ$ [26]. The theoretically predicted value $u \simeq -0.196\text{A}^\circ$ is in the excellent agreement with that. It should also be mentioned that the calculation based on the crystal lattice

static theory [22] gives the same equation for displacement if the phonon spectrum dispersion is neglected.

The matrix u^*_{ij} given by (37) also predicts that the crystal lattice parameters of GP zone in (001) plane are exactly the same as in Al matrix.

b. <u>θ" Phase</u>

Aging above 100°C results in dissolution of GP zones and appearance of platelets of θ" metastable phase that is formed by alternation of Cu and AL (001) planes in the fcc lattice Cu Al Al Al Cu Al Al Al... Therefore atomic fraction of Cu in θ" phase is Cp=1/4. The θ" phase formed due to such a sequence is a tetragonal phase with $c \tilde{=} 2a_{sc}$ and $a \tilde{=} a_u$ θ" phase being an ordered fcc-based superstructure enriched by Cu atoms has misfit described by eq.(37) and therefore should also be formed as platelike precipitates with {100} habit.

Let us calculate the θ" phase crystal lattice parameters using eq. (37). It predicts

$$c = (1+u^*_{33})\ 2a_{Al} = 1 + \left(\frac{c_{11}+2c_{12}}{c_{11}}\right)\left(\frac{da}{adc}\right) \cdot (1/4) \cdot 2 \cdot 4.04$$

$$= \left[1 + \frac{1.068+2\cdot 0.607 \cdot (-0.091)\ 1/4}{1.068}\right] \cdot 2 \cdot 4.041 = 7.69\ A^\circ$$

Since the parameters of the constraint θ" phase in the (001) habit plane should be exactly the same as in the matrix, we predict

$$a = a_{Al} = 4.041\ A^\circ$$

The calculated values c=7.69A° and a=4.041A° are perfectly matched to the observed crystal lattice parameters c=7.7A° and a=4.04A°. Therefore both the habit plane orientation and crystal lattice parameters of θ" fit very well the theoretical predictions.

c. <u>θ′ Phase</u>

The intermediate tetragonal θ′ phase that succeeds the θ″ phase in the course of aging has the fcc-faced lattice $Al_2Cu\square$, where $\square$ designates vacancy. The presence of built-in vacancies in the fcc lattice of the θ′ phase introduce the additional contraction to the stress-free transformation strain. The theory predicts that θ′ phase precipitates should also be platelets with the {001} habit. This conclusion is in agreement with electron microscopic observation.

Since crystal lattice mismatch for θ′ phase in the Al matrix cannot be determined at the moment (we only know that its dilatational part is much larger than for the θ″ phase), we cannot calculate parameter c using the same equation as with the θ″ phase. However, the theory predicts that the crystal lattice parameter, a, which is situated in the habit plane must coincide exactly with the crystal lattice parameter of pure Al, i.e., $a_{Al}=4.041A^{\circ}$. This prediction is also in excellent agreement with the observed results:

$$a_{\theta'} = 4.04\ A^{\circ}$$

$$c_{\theta'} \geqslant 5.8A^{\circ}$$

d. <u>GP Zones with Small Crystal Lattice Mismatch</u>

GP zones were also observed in Cu-Co, Al-Zn, Al-Ag alloys. The difference between atomic diameters os solute and solvent atoms for them is less than about 3%. Since the GP zone volume is small, the theory predicts spherical shape of precipitates (see section 4). This is in agreement with x-ray and electron microscopic observations. It is of interest to note that estimations of the elastic moduli of the precipitate phase in Al-Zn alloys gives $c_{11}-c_{12}-2c_{44} > 0$ [27]. In this situation the theory developed above predicts spherical shape in the early

stage of aging which should be transformed into octahedron (or tetrahedron) and later into {111} platelets.

e. GP Zones When Precipitate Phase Is Hexagonal

Calculations by Mayo and Tsakalakos for GP zones and metastable η' hexagonal phase give the $\{111\}_{Al}$ habit [11] which is in agreement with electron microscopic observation. Precipitates of the η' metastable hexagonal phase in Al-Zn-Mg alloys give one more confirmation that a coherent plate-like precipitate and matrix have exactly the same crystal lattice parameters in the habit plane. Crystal lattice parameters of constraint hexagonal η' phase are

$$a_{\eta'} = 4.96\text{A}^{\circ}, \quad c_{\eta'} = 8.68\text{A}^{\circ}$$

The Al-based matrix has the parameter $a_0=4.054\text{A}^{\circ}$. The $[\bar{1}/2\ \bar{1}/2\ 1]_0$ and $[\bar{1}/2\ \ 1\ \bar{1}/2]_0$ translations of the fcc matrix lying in the (111) plane which are transformed into the parameter $a_{\eta'}$ of the η' phase are equal to

$$T([\bar{1}/2\ \bar{1}/2\ 1]) = T([\bar{1}/2\ 1\ \bar{1}/2]) = a_0\sqrt{3}/2 = 4.054 \cdot \sqrt{3}/2 = 4.965\text{A}^{\circ}.$$

This value with accuracy of x-ray measurements coincides with the value $a=4.96\text{A}^{\circ}$ observed.

B. Precipitation of Nitrides in Fe-N Alloys

Elastic strain theory formulated above can be applied to determine morphology and crystal lattice correspondence of nitride precipitates in Fe-N martensite [9,22].

a. Precipitates of α'' Phase ($Fe_{16}N_2$) in Fe-N Martensite

The decomposition reaction that occurs in tempered bct Fe-N martensite leads to the formation of ordered bcc-based tetragonal nitride, $Fe_{16}N_2$ (α'') in the bcc αFe matrix which later transforms into

fcc-based γ' phase (Fe_4N). According to Jack [28], α'' phase is a tetragonal phase with

$$a(\alpha'') = 2a_{Fe} = 2.2.86 = 5.72A^{\circ}$$

$$c(\alpha'') = 6.292A^{\circ} \sim 2a_{o}$$

The spacing $a(\alpha'')$ is exactly equal to twice the crystal lattice parameters of the αFe. This coincidence cannot be accidental. It may be explained if α'' phase precipitates are coherent platelets with the (001) habit. Then the theory predicts that parameter $a(\alpha'')$ situated in the habit plane (001) should be exactly equal to the corresponding parameter $2a_{Fe}$ of the (001) matrix plane. In other words, the crystal lattice parameters observed by Jack are parameters of constraint precipitate. This conclusion which directly follows from the theory was proved by the crystal lattice parameter measurements of the single phase ordered α'' phase solid solution which is, by definition, the stress-free Fe-8.56 at%N single phase alloy for the measured crystal lattice parameters are

$$a(\alpha'') = 5.692\ A^{\circ}$$

$$c(\alpha'') = 6.180\ A^{\circ} \quad [29]$$

For this alloy $a(\alpha'') \neq 2a_{Fe}$ which proves that coincidence of $a(\alpha'')$ with $2a_{Fe}$ observed by Jack is a result of constraint. For the stoichiometric alloy the stress-free strain is $\varepsilon^{\circ}_{11} = -0.006537$, $\varepsilon^{\circ}_{33} = 0.107397$. These values enables one to calculate the crystal lattice parameters of the constraint (001) precipitate using eq.(29). The calculation gives

$$a(\alpha'') = 2a_{Fe} = 2 \cdot 2.80 = 5.720\ A^{\circ}$$

$$c(\alpha'') = 6.289\ A^{\circ}$$

which is in excellent agreement with the Jack observations.

$$t = \frac{-0.004895}{0.080413} = -0.0608$$

In the case of the (001) habit the constraint strain (29) has the form

$$u^{*}_{ij} = \varepsilon^{\circ}_{33} + \frac{2c_{12}}{c_{11}}\,\varepsilon^{\circ}_{11} \begin{pmatrix} 000 \\ 000 \\ 001 \end{pmatrix}$$

ordered phase Fe_4 [28]. The crystal lattice parameter of the γ' phase near its stability limit is

$$a_{\gamma'} = 3.791\ A^{\circ}$$

whereas, that of the bcc αFe matrix is

$$a_{\circ} = 2.860\ A^{\circ}$$

Since the stress-free transformation strain for bcc -> fcc crystal lattice rearrangement is the tetragonal Bain strain, its components are

$$\varepsilon^{\circ}_{11} = \varepsilon^{\circ}_{22} = a_{\gamma'}/a_{\circ}\sqrt{2}) - 1 = (3.791/2.86\sqrt{2}) - 1 = -0.0627$$

$$\varepsilon^{\circ}_{33} = a_{\gamma'}/a_{\circ}) - 1 = (3.791/2.86) - 1 = 0.3255$$

$$t = \varepsilon^{\circ}_{11}/\varepsilon^{\circ}_{3}) = -0.1926$$

With this numerical value t = -0.1926 using the elastic constants of pure iron in eq.(25a) we have

$$n_{\circ} = (0.484,\ 0,\ 0.875)_{bcc}$$

This unit vector is normal to the predicted habit plane which deviates only by 2.4° from the $(102)_{bcc}$ habit observed [31]. Making use of the elastic constants of αFe and value t = -0.0608 in eq.(25a) yields the vector $n_{\circ}$ minimizing B(n) in the form

$n^{\circ} = (\sin\theta,\ 0,\ \cos\theta)$ where $\theta = 18.6^{\circ}$ or $n^{\circ} = (0.279,\ 0,\ 0.960)$ which is a deviate less than 1° from the normal to the $(207)_{bcc}$ plane. Therefore a large coherent precipitate of the α'' phase whose shape is predominantly dictated by the elastic energy relaxation should be

produced in the form of a thin plate with habit close to $(207)_{bcc}$ [22]. When this result was first obtained there was the impression that it contradicts the electron microscopic observations of the α" phase in the form of a thin plate with (001) habit. However, using the same theory Hong, et al. have demonstrated that for a small α" phase precipitate whose equilibrium aspect ratio is less than 11, the habit plane is $(001)_{bcc}$ [9]. Only later with particle coarsening should it be transformed to the (207) habit. The electron microscopic observations seem to confirm this prediction. The (001) habit plane was observed to be transformed into puckered (001) plane composed of segments of planes close to the {207} planes [30].

C. Habit Plane of β-Phase in V-H Alloys.

β phase in vanadium hydride is an interstitial bcc-based solid solution with H atom occupying the sole Oz octahedral sublattice of bcc V host lattice. Such an occupancy produces pseudotetragonal distortion. β phase crystal lattice parameters are

$$a = 3.002\ A^{\circ} \quad C = 3.311\ A^{\circ}$$

The V matrix lattice has the parameter

$$a_0 = 3.032\ A^{\circ}$$

Therefore, the stress-free transformation strain is

$$\varepsilon^{p}_{11} = = -0.0099 \quad \varepsilon^{\circ}_{3,3} = 0.0890 \text{ and } t = -0.111$$

With the V elastic constants eq.(25b) yields

$$n_0 = (0.277,\ 0.277,\ 0.920)$$

which is close to the normal to the $(227)_{bcc}$ habit. The normal to the observed habit plane of the β phase is

$$n_{obs} = (0.293,\ 0.236,\ 0.926)\ [37,38]$$

Deviation of calculated habit from the observed one is about 0.9°. This

agreement can be regarded as very good because the theory does not have any filtering parameters.

6. Magnetostatic Energy and Analogy with Elastic Strain Energy.

As was mentioned in the Introduction there is the profound analogy between elastic strain energy of a two-phase coherent dispersoid and magnetostatic energy of ferromagnets and electrostatic energy of ferroelectrics. The consequences of this analogy are so important that they deserve a special discussion. Below the equation for magnetostatic energy of the system of ferromagnetic domains will be described, and it will be shown that mathematically the equation for magnetostatic energy is analogous to one for the elastic strain energy. It will be demonstrated that the k-space technique developed above for the elastic energy can be with the same efficiency applied for magnetostatic energy of ferromagnets in the cases when the Bloch wall thickness is well below the typical size of domains [22].

As is known, the magnetostatic energy may always be represented as the sum of interacting magnetic dipoles

$$E_{mag} = 1/2 \iint d^3r d^3r' m(r)_i \left[\frac{\delta_{ij}}{|r-r'|^3} - 3 \frac{(r-r')_i (r-r')_j}{|r-r'|^5} \right] m(r')_j \quad (40)$$

where $m(r)$ is the magnetization density at the point r, the integration in (40) is taken over the infinite crystal body. Using the Fourier representations:

$$m(r) = \int \frac{d^3k}{(2\pi)^3} M(k) \exp(ikr)$$

$$r^{-3}\delta_{ij} - r^{-5}\, 3r_i r_j = 4\pi \int (k_i k_j / k^2) * \exp(ikr)\, d^3k/(2\pi)^3$$

in (37) one has

$$E_{mag} = (1/2) \iiint_{-\infty}^{\infty} 4\pi \frac{|M(k)k|^2}{k^2} d^3k/(2\pi)^3 \quad (41)$$

where for simplicity the magnetic susceptibility is assumed to be equal to unity.

Let us consider an arbitrary system of ferromagnetic particles with various possible directions of magnetization designated by the index p. Then the spatial distribution of the magnetization produced by the system of magnetic particles or magnetic domains is

$$\mathbf{m}(\mathbf{r}) = M_0 \sum \mathbf{e}(p)\, \tilde{\theta}(p,\mathbf{r}) \qquad (42)$$

(compare with eq.(6), where $\tilde{\theta}(p,\mathbf{r})$ is again the shape function of domains of the p^{th} type, $\mathbf{e}(p)$ is the unit vector along the magnetization direction of p^{th} domains. The Fourier transform of (42) is

$$\mathbf{M}(\mathbf{k}) = M_0 \sum \mathbf{e}(p)\, \theta(p,\mathbf{k})$$

substituting this equation to (41) yields

$$E_{mag} = 2\pi M_0^2 \sum_{p,q} \int B(\mathbf{k}/k)^{mag}_{pq}\, \theta(p,\mathbf{k})\, \theta(q,\mathbf{k})^*\, d^3k/(2\pi)^3 \qquad (43)$$

where

$$B(\mathbf{n})^{mag}_{pq} = (\mathbf{e}(p)\mathbf{n})(\mathbf{e}(q)\mathbf{n})$$

is the angular function of the $\mathbf{k}$ vector direction, $\mathbf{n} = \mathbf{k}/k$. One may readily see that eq.(43) for the magnetostatic energy has absolutely the same form as eq.(14) for the elastic energy.

For a single domain particle eq.(43) gives the analog of eq.(15) for the elastic energy of a single coherent inclusion:

$$E_{mag} = 2\pi M_0^2 \int B(\mathbf{k}/k)_{mag}\, |\theta(\mathbf{k})|^2\, d^3k/(2\pi)^3 \qquad (44)$$

where $B(\mathbf{n}) = (\mathbf{en})^2$. Equation (44) can also be rewritten as

$$E_{mag} = 2\pi M_0^2 \alpha\, V$$

where

$$\alpha = V^{-1} \int [(\mathbf{ek})^2/k^2] |\theta(\mathbf{k})|^2\, d^3k/(2\pi)^3$$

is the k-space representation for the so-called demagnetization factor, the dimensionless coefficient depending only on the shape of the particle.

It should be emphasized that eq.(43) gives the close solution for an arbitrary set of ferromagnetic domains whose size is well above the Bloch wall thickness. This equation can be efficiently used for calculation of the reverse magnetization and for analysis of morphologies of domain structures. To the authors knowledge, this k-space formulation of the magnetostatic energy is new and can be very useful in various applications because of its mathematical simplicity.

The formal analogy between the elastic energy (14) and (15), and the magnetostatic energy (43) and (44) consists in the fact that both have the same mathematical form. The kernel function $B(\mathbf{k}/k)_{pq}$ in the elastic energy (14) as well as the corresponding kernel function $B(\mathbf{k}/k)^{mag}_{pq}$ depend on the direction of the wave vector $\mathbf{k}$ rather than on its absolute value. The kernel functions $B(\mathbf{k}/k)_{pq}$ are, in fact, the Fourier transform of the pairwise interaction between elements of volume of the domains (or coherent particles) of the type p and q. These energies can be found by the back Fourier transform which gives the singular function

$$V_{pq}(r-r') = 1/|r-r'|^3 \quad \Psi\,((r - r')/|r - r'|)$$

where $\Psi(\mathbf{m})$ is the function of the direction, $(r-r')/|r-r'|$. This is the typical form of the dipole-dipole like interaction. The elastic interaction between elements of coherent precipitate volume has exactly the same the form of the dipole-dipole interaction when B(n) has the cylindrical symmetry about a certain axis e, i.e. when

$$B(n) = B(ne) \cong \max B(n) + \beta(ne)^2 + \ldots$$

Then the back Fourier transform yields

$$V(r-r') = \beta|r-r'|^{-3}\,[1-3\,((r-r')e)^2/|r-r'|^2\,]$$

which corresponds to interaction between two dipoles, $\sqrt{\beta}e$, separated by the distance $\mathbf{r}-\mathbf{r}'$.

The major physical consequence of the fact that $B(k/k)^{mag}_{pq}$ depends only on direction of $\mathbf{k}$ vector is the well known effect, dependence of the magnetostatic energy on morphology of ferromagnetic particles. It results in instability of a homogeneous state of the ferromagnetic phase with respect to decomposition into the system of domains. In the case of a uniaxial ferromagnet film a large domain with the opposite magnetization direction than the matrix also proves to be unstable with respect to splitting into the array of bubble domains. The reason for this is the same, repulsion between volume elements of the domain which repel each other as parallel identical dipoles.

Summing up the foregoing one can see that instability of a homogeneous state of ferromagnet (and ferroelectric) is caused by the fact that the magnetostatic energy of a ferromagnetic phase unlike the exchange energy depends not only on the volume of the phase, but also on its morphology, shape and spatial distribution. It will be shown below that the same is true for the elastic eneergy of a coherent dispersoid.

7. Strain-Induced Instability of Coherent Particles in Two-Phase Cubic Alloys.

The elastic energy, unlike the "chemical" free energy of a two-phase alloy depends not only on the precipitate phase volume, but also on its shape and spatial distribution. The situation here is the same as with magnetostatic energy. Therefore, one could expect that dependence of elastic energy on morphology would produce the same effect, viz. instability of large coherent particles. This instability, splitting large coherent precipitates, analogous to the splitting

instability resulting in formation of bubble domains would seriously affect the traditional concepts of coarsening in two-phase cubic alloys. The main result of the conventional theory of coarsening, that a two-phase alloy becomes more stable upon coarsening should be questioned.

First of all, all studies concerning evolution of alloy upon coarsening implicitly assume that precipitates remain intact and, if they coarsen, just monotonically increase their size. The theory [2,4] enables us to test this assumption. Following [32] we shall demonstrate that when a cuboidal particle of a cubic phase precipitate reaches a certain critical size, multiple of the typical length r_0 introduced above by eq.(36), the cuboid becomes unstable and decomposes into a doublet and later into an octet of subparticles. This phenomenon reflects repulsive interaction between elements of volume of a cuboid which, in fact, opposes the coarsening. Similarly we can predict that large plate should also be unstable with respect to splitting into several subplates and so on.

Splitting is not the only way to prevent formation of too large overgrown precipitates. Elastic interaction between them may produce the same effect. This interaction would just oppose coarsening, the phenomenon which was really observed.

To analyze the elastic energy change upon transition of a monlytic precipitate into a group of subparticles we should compare the elastic energies of both states. To do this, let us represent the shape function, $\theta(\mathbf{r})$ of a group of identical subparticles as the sum of their shape functions, $\tilde{\theta}_0(\mathbf{r}-\mathbf{R}_j)$

$$\tilde{\theta}(\mathbf{r}) = \Sigma_j \, \theta_0(\mathbf{r}-\mathbf{R}_j)$$

where the index j labels all subparticles $\mathbf{R}_j$ describes the position of

the center of gravity of the j^{th} subparticle. The Fourier transform of this function is

$$\theta(\mathbf{k}) = \theta_0(\mathbf{k}) \Sigma_j \exp(-i\mathbf{k}\mathbf{R}_j) \qquad (45)$$

where the mutual location of precipitates is taken into account by the "structural factor," $\Sigma_j \exp(-i\mathbf{k}\mathbf{R}_j)$, $\theta_0(\mathbf{k})$ is the Fourier transform of the shape function of a subparticle.

Substituting (45) to (15) gives the close equation for the elastic energy of this group of precipitates:

$$E = 1/2 \int B(\mathbf{k}/k) |\theta_0(\mathbf{k})|^2 |\Sigma_j \exp(-i\mathbf{k}\mathbf{R}_j)|^2 \, d^3k/(2\pi)^3 \qquad (46)$$

Using the expansion of the function B(n) in the series of cubic harmonics and terminating the corresponding series by two forms, we have

$$E = E_0 V + E_1 V \, 4[I_1 + 27\mu I_2/2]$$

where E_0 and E_1 are given in comments to eq.(34),

$$\mu = (c_{11} - c_{12} - 2c_{44})/(c_{11} + 2c_{12} + 4c_{44})$$

The dimensionless coeff icients I_1 and I_2 have the form

$$I_1 = V^{-1} \int \gamma_1(\mathbf{k}/k) \, |\theta_0(\mathbf{k})|^2 \, |\Sigma_j \exp(-i\mathbf{k}\mathbf{R}_j)|^2 \, d^3k/(2\pi)^3$$

$$I_2 = V^{-1} \int \gamma_2(\mathbf{k}/k) \, |\theta_0(\mathbf{k})|^2 \, |\Sigma_j \exp(-i\mathbf{k}\mathbf{R}_j)|^2 \, d^3k/(2\pi)^3 \qquad (47)$$

where $\gamma_1(\mathbf{n}) = n_x^2 n_y^2 + n_x^2 n_z^2 + n_y^2 n_z$

$\gamma_2(\mathbf{n}) = n_x^2 n_y^2 n_z^2$,

(n_x, n_y, n_z) are Cartesian components of the unit vector $\mathbf{n}$. The constants I_1 and I_2 are geometrical factors which depend on shape and mutual location of subparticles. Numerical calculations of the integrals (47) at $c_{11}-c_{12}-2c_{44} < 0$ show that a cuboidal particle has greater elastic energy than an octet of cuboidal subparticles, the energy of the octet being the lowest when cuboidal subparticles are separated by the distance $u \simeq 0.4a$ where $2a = \sqrt[3]{V}$ is the edge length of the initial cuboid (Fig. 2). The cuboid subparticle has also the greater elastic energy than

the doublet of the identical parallelopiped subparticles formed due to splitting the cuboid. The lowest energy of the doublet is attained when separation distance between subparticles is 0.8a (Fig. 3). The elastic energy of the octet is less than that of the doublet of the same volume(Fig 4). As for the interphase energy, its increase is caused by the formation of new interphase because splitting is less for the doublet than for the octet. Therefore, for a smaller precipitate when the interphase energy contribution dominates, a doublet should be expected. For the layer precipitate when the elastic energy prevails, the octet is favored. The numerical caluculation and comparison of the elastic and surface energies of both morphologies show that the cuboid -> doublet transformation may occur when $\sqrt[3]{V} \geqslant 27r_0$ where V is the cuboid volume, r_0 is given by eq.(36). Doublet -> octet transformation may occur when $\sqrt[3]{V} \leqslant 82r_0$. At greater volumes the octet ceases to be stable with respect to transformation to a platelet. These results naturally fit the results in section 4 concerning the shape transformaiton of a monolitic particle from a spheroic to a cuboid which occurs when $\sqrt[3]{V} \leqslant 7.6r_0$. Together these results confirm our qualitative conclusions formulated above that the morphology transformation is determined by the ratio between the efficient particle size $\sqrt[3]{V}$ and characteristic length r_0 depending on interphase energy, crystal lattice misfit and elastic moduli. The $\sqrt[3]{V}/r_0$ ratio, in fact, is the measure of contribution of elastic energy with respect to interphase energy to the coarsening process. The more is this ratio, the more contribution of elastic energy.

The stability limits found above characterize the conditions when one morphology becomes energetically more favorable than another. However, it should be emphasized that the "overgrown" microstructure is

not automatically transformed into another. It may still be stable with respect infinitesimal variations of the shape. In this situation the overgrown microstructure is metastable. It can be transformed into the stable one only by the finite shape transformation playing the same role as the critical nucleus fluctuation in the conventional phase transformation thermodynamics. Since the critical shape fluctuation required for the shape transformation is macroscopically large, all metastable morphologies should be very stable and transform into the stable morphology only near the metastability limit where a metastable particle also becomes unstable with respect to infinitesimal shape variations.

Simple qualitative interpretation of the microstructure transformation, spheroid->cuboid->doublet->octet->platelet, upon coarsening is the following. In the relevant case when $c_{11}-c_{12}-2c_{44} < 0$ elements of the precipitate phase volume repel each other along the <111> directions. This repulsion transforms a spheroid into cuboid due to stretching of the spheroid volume along the <111> directions. The same effect results in splitting the cuboid along the same <111> direction transforming the cuboid into an octet. The only reason why new phase precipitates can exist as monolitic homogeneous particles is the interphase energy effect. The interphase energy opposes the splitting since it produces new interphase. The situation here is the same as in the case of ferromagnets, because both elastic energy and magnetostatic energies destroy the homogeneous state of a particle in the zero interphase energy limit, or in the limit of large particle volume when interphase energy plays the minor role. The example of such a behaviour gives a strip ferromagntic domain which becomes unstable with respect to splitting into the set of bubble domains because of repulsion between the elements of the strip

domain volume repelling each other as parallel magnetic diploes.

The above results show that the mathemetically simple theory based on the homogeneous modulus case approximaiton can be efficiently applied to the important techincal alloys. For example, it has been shown above in section 3F that the homogeneous modulus approximation gives nevertheless asymptotically exact value of the elastic energy of platelike precipitates if the elastic moduli of the precipitate phase are used. The reason for that is the concentration of elastic strain within the platelike particle (the ratio of elastic energy concentrated out side and inside the particle tends to zero as the squared aspect ratio $(D/L)^2$ -> 0, where D is the thickness, L is the length of the particle). On the other hand, equations for the edge energy of the plate in section 3E are also a symptocially correct if elastic moduli of the matrix are used. The reason for that is the same. The edge energy is the one that is concentrated in the matrix with the same asymptotic accuracy $(d/L)^2 \rightarrow$ $\rightarrow$ 0. Therefore, all results concerning the habit plane, eigenstrain and orientational relations obtained in section 3 in the homogeneous modulus approximation proves to be valid if the moduli are different. In fact, reduction of elastic energy upon strain-induced stage of coarasening occurs mainly due to redistribution of elastic strain from the matrix to the precipitate phase so that ultimately all elastic strain proves to be contained in thin plate particles. In limit case of the martensite-like optimal structure at which bulk elastic energy completely vanishes, the value of elastic moduli does not matter at all. This is the reason why pure crystallographic theory of martensitic transformation proved to be so efficient.

ACKNOWLEDGMENTS

This work is supported by the Director, Office of Energy Research, Office of Basic Energy Science, Materials Sciences Division of the U.S. Department of Energy under contract υDe-Ac0376Sf00098.

REFERENCES

1. J.D. Eshelby, Proc. Roy. Soc., A241, 376 (1957); A252, 56 (1959); Prog. Solid Mech., 2, 89 (1961)
2. A.G. Khachaturyan, Soviet Physics - Solid State, 8, 2710 (1966)
3. A.L. Roytburd, Kristallography, 12, 567 (1967)
4. A.G. Khachaturyan and G.A. Shatalov, Soviet Physics - Solid State, 11, 118 (1969)
5. S. Wen, A.G. Khachaturyan, J.W. Morris, Jr., Proc. Int. Symp. Modulated Struct., AIP, N.Y. (1979) p. 168; Proc. Int. Conf. Martensitic Transormation, Cambridge, Mass, (1979) p. 94; Metallurgical Transactions 12A, 581 (1981)
6. J.W. Wert, Acta Metallurgica, 24 65 (1976)
7. M. Hong, M.S. Thesis, University of California, Berkeley, CA, (1978)
8. J.K. Lee and W.C. Johnson, Phys. Stat. Solidi 46(a), 375 (1976)
9. M. Hong, D.E. Wedge and J.W. Morris, Jr., Acta Metallurgica, 32, 279 (1984)
10. A.L. Roitburd and N.S. Kosenko, Phys. Stat. Solidi, 35(a), 735 (1976)
11. W.E. Mayo and T. Tsakalakos, Metallurical Transactions, 11A, 1631 (1980)
12. S.H. Wen, E. Kostlan, M. Hong, A.G. Khachaturyan, J.W. Morris, Jr., Acta Metallurgica, 29, 124 (1981)

13. V. Lanteri, T.E. Mitchell and A.H. Heuer, Journal of American Ceramics Society, 69, 564 (1986)

14. A.G. Khachaturyan and G.A. Shatalov, Soviet Physics - JETP, 29, 557 (1969)

15. A.G. Khachaturyan, "The Theory of Phase Transformations and Structure of solid Solutions", Moscow, Nanka (1974); Soviet Physics - JETP, 31, 98 (1970); Phys. Stat. Solidi, 35, 119 (1969)

16. A.G. Khachaturyan, V.N. Aizapetyan, Phys. Stat. Solidi, (a)26, 61 (1974)

17. E. Seitz and D. de Fontaine, Acta Metallurgica, 26, 1671 (1978)

18. H. Yamunchi and D. de Fontaine, Acta Metallurgica, 27, 763 (1979)

19. J.K. Lee, D.M. Barnett, and H.I. Aaronson, Metallurgical Transactions, 8A, 1447 (1977)

20. L.J. Valpole, Proc. Roy. Soc. (A)300, 270 (1967)

21. J.R. Willis, "Asymmetric Problems of Elasticity", Adam Prize Essay, University of Cambridge, (1970)

22. A.G. Khachaturyan, "The Theory of Structural Transformations in Solids", Wiley β Sons, N.Y., (1983)

23. J. Gjonnes, Chr. J. Simensen, Acta Metallurgica, 18, 881 (1970)

24. G. Thomas and J. Nutting, Journal of Inst. Metals, 88, 81 (1959-60)

25. V. Gerold, Acta Cryst. 11, 236 (1958)

26. K. Doi, Acta Cryst. 13, 45 (1960)

27. V. Gerold, in Proc. of 116 TMS Meeting, Denver, Colorado, February 23-26, 1987

28. K.H. Jack, Proc. Roy. Soc. (A)208, 216 (1951)

29. A.V. Suyazov, M.P. Usikov and R.M. Mogutnov, Fit. Met. Metalloved, 42, 755 (1976)

30. P. Ferguson, V. Dahmen and K.H. Westmacott, Scripta Metallurica, 18, 57 (1984)

31. M.P. Usikov and A.G. Khachaturyan, Phys. Met. Metallography, 30, G14 (1970)

32. A.G. Khachaturyan, S.V. Semenovshaya, and J.W. Morris, Jr., (submitted to Acta Metallurica)

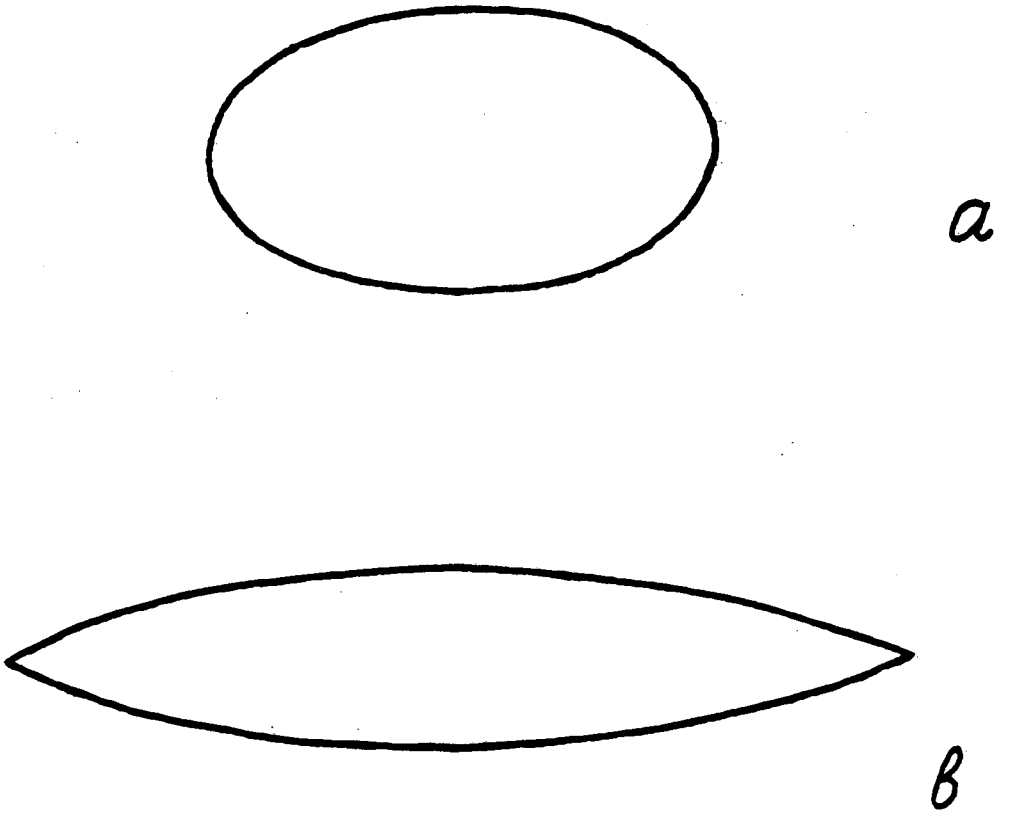

Fig. 1 Calculated optimal shape of the platelet particle in the habit plane.

(a) slightly anisotropic case (oval shape)
(b) strongly anisotropic case (lense shape)

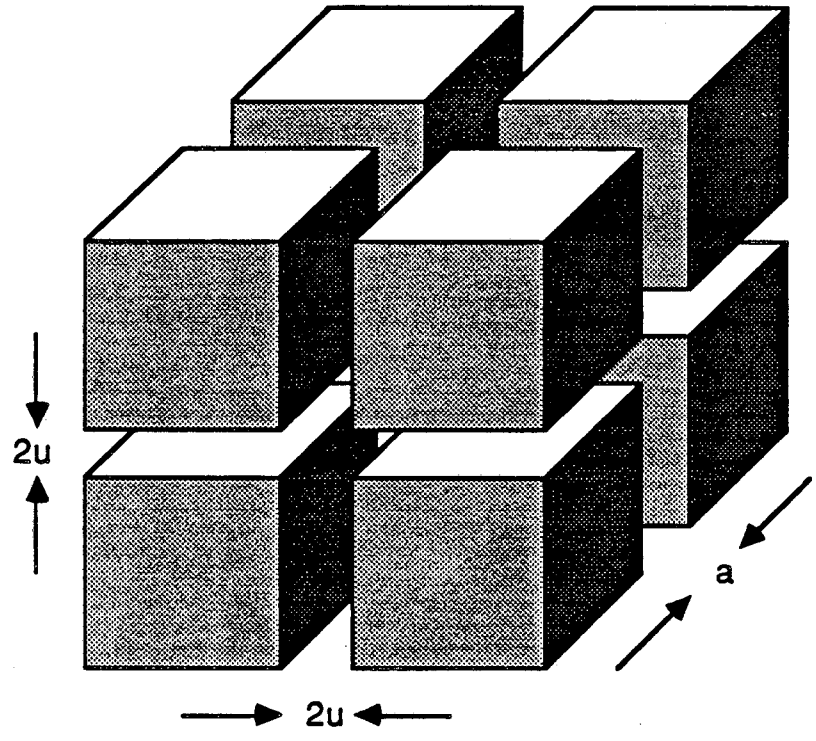

Fig. 2 Schematic drawing of octet that results from the decomposition of a cuboidal particle.

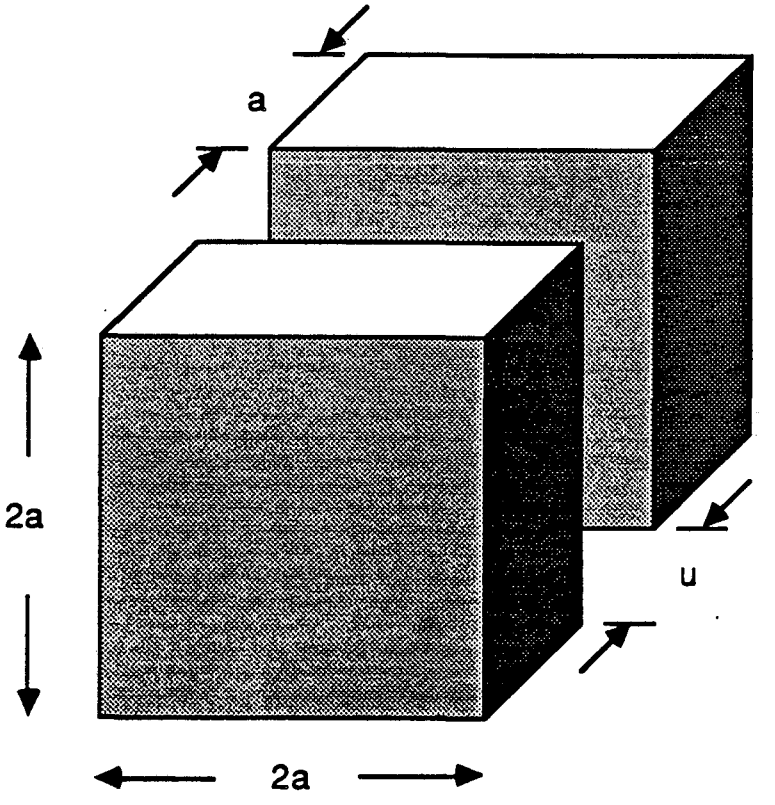

Fig. 3 Schematic drawing of doublet of plates that results from the decomposition of a cuboidal particle.

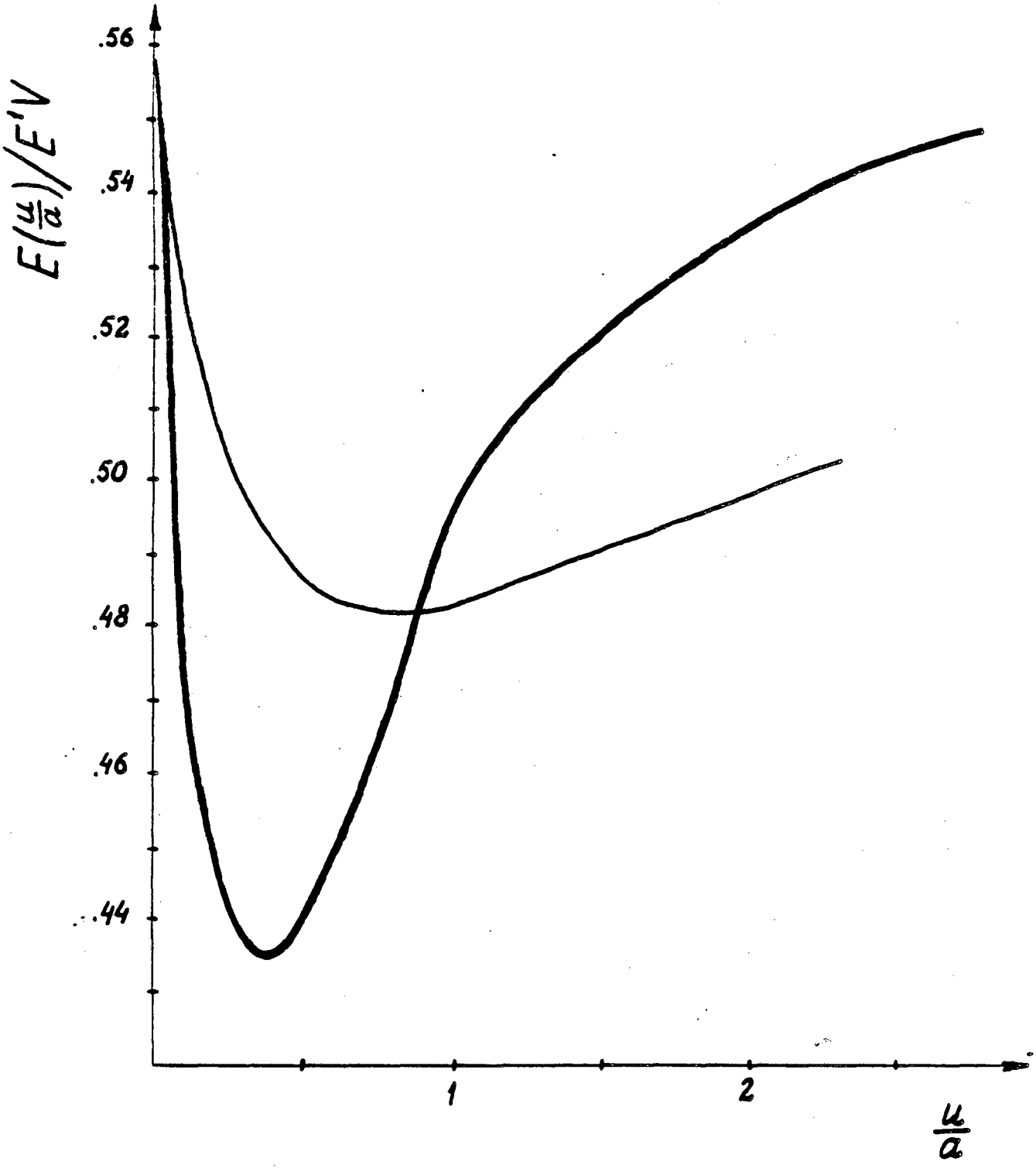

Fig. 4 Configurational elastic energy, in dimensionless form, as a function of dimensionless particle spacing (u/a) for an octet of cubes (dark line) and a doublet of plates (light line).

LAWRENCE BERKELEY LABORATORY
TECHNICAL INFORMATION DEPARTMENT
UNIVERSITY OF CALIFORNIA
BERKELEY, CALIFORNIA 94720